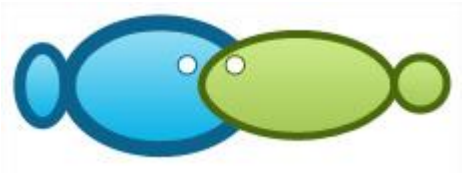

Predicting drug-likeness properties of small molecules from yellow tomalley hydrolysate of blue swimming crab (*Portunus pelagicus*)

[1]Putut H. Riyadi, [1]Eko Susanto, [1]Apri D. Anggo, [2]Mochammad F. Atho'illah, [2]Muhaimin Rifa'i

[1] Department of Fish Products Technology, Faculty of Fisheries and Marine Sciences, Diponegoro University, Semarang, Central Java, Indonesia; [2] Department of Biology, Faculty of Mathematics and Natural Sciences, Brawijaya University, Malang, East Java, Indonesia. Corresponding author: P. H. Riyadi, putut.riyadi@live.undip.ac.id

Abstract. Blue swimming crab (*Portunus pelagicus*) is a valuable commodity in high demand, as is their waste products. Hydrolysis methods can be used to extract the protein content of the blue swimming crab. The current study aimed to explore the potential of yellow tomalley hydrolysate of blue swimming crab as an antihypertensive agent with an *in silico* approach. Gas Chromatography-Mass Spectrometry was used to identify the bioactive compounds in the yellow tomalley hydrolysate of blue swimming crab (YTHBSC). Nine bioactive compounds found from YTHBSC were then analyzed for antihypertensive-related activity using the Prediction of Activity Spectra for Substances (PASS) server. Furthermore, the SwissADME web server and ProTox II were used to evaluate drug-likeness, excretion, metabolism, distribution, absorption, and toxicity of the small molecule from YTHBSC based on PASS online prediction. There were eight compounds found in YTHBSC related to antihypertensive properties. Furthermore, 6 of 8 small molecules of YTHBSC have good bioavailability based on SwissADME analysis. Except for N,N-dimethyl-methanamine, the YTHBSC small molecules followed the Lipinski rules and had high gastrointestinal (GI) absorption values. YTHBSC's small molecules have the potential to act as antihypertensive agents.

Key Words: antihypertensive, *in silico*, waste product.

Introduction. Blue swimming crab (*Portunus pelagicus*) has a great economic value in Indonesia and is one of the five primary commodities with the highest export value. Based on Statistics Indonesia (2021), in 2020, the export value of crustaceans, including crabs and other invertebrates, reached 305704251.01 USD, with a volume of 66236.49 tons. In 2021, the export value of crustacea increased to 366880868.22 USD, with a volume of 76993 tons (Statistics Indonesia 2021). The increase in exports results in increased by-products, including solid waste (shells or skins) and liquid waste. The waste can impact the environment (Chang & Lee 2019).

Blue swimming crab (BSC) waste generated from industrial processes consists of solid and liquid waste (Riyadi et al 2020a). The yellow tomalley, a solid waste of the BSC canned industry, is a yellowish substance found under the surface of the crab shell. This ingredient has a taste resembling crab meat and has high protein content. Therefore, it can be used as hydrolysate (Sasongko et al 2018). One of the efforts in processing fishery waste is producing protein hydrolysate (Gao et al 2021). Protein hydrolysate is a by-product of chemical or enzymatic hydrolysis that converts proteins into simple peptides and amino acids (Zamora-Sillero et al 2018). Enzymatic hydrolysis has several advantages over chemical hydrolysis, including no sugar degradation resulting from hydrolysis, softer process conditions (neutral pH, low temperature and pressure), and the enzymatic process is environmentally friendly (Vijaykrishnaraj & Prabhasankar 2015).

High blood pressure is one of the diseases that globally causes many deaths (Mills et al 2020). Hypertension can also lead to cardiac hypertrophy, cardiovascular disease, aortic rupture, and renal failure (Mensah 2016). Several studies have shown that

products made from fish waste have antihypertensive activity, such as northern shrimp (*Pandalus borealis*) by-products (Kim et al 2016a) and tilapia viscera (Riyadi et al 2020b; Riyadi et al 2021a). Bioinformatics and *in silico* analyses play a pivotal role in quickly designing, screening, and developing therapeutic drugs (Zloh & Kirton 2018). PASS has been a useful website for predicting biological spectral activity since 2000. Computer models can predict biological activity in published and new compounds, allowing for early screening of unpromising molecules. Computer-assisted simulations of drug excretion, metabolism, distribution, and absorption are being studied to apply an anticipatory and trustworthy data complement to experimental accessions. The pharmacokinetics, physicochemical, and pharmacological characteristics of small compounds are predicted using this computational model (Sliwoski et al 2014). SwissADME is a comprehensive and integrated website from the Swiss Institute of Bioinformatics (SIB), which offers bioinformatics recourses to researchers worldwide (Ndombera et al 2019).

To the best of our knowledge, the application of BSC waste as an alternative treatment for hypertension is limited. Therefore, this study aimed to explore the potential of yellow tomalley of BSC hydrolysate as an antihypertensive agent. This study uses computational analysis to evaluate and predict biological potential, drug-likeness, excretion, metabolism, distribution, absorption, and toxicity of yellow tomalley hydrolysate of BSC.

Material and Method

Production of the yellow tomalley hydrolysate of BSC. Protein hydrolysate was made by an enzymatic hydrolysis reaction using the alcalase enzyme. The protein hydrolysate production was according to the Riyadi et al (2019) method. The yellow tomalley of BSC collected from a small-scale industry of pasteurized BSC was homogenized with aquadest in a ratio of 1:2. The alcalase enzyme (Sigma-Aldrich) was added at a concentration of 1.5%. The hydrolysis process was performed for 2 h in a water bath at 55°C. The pH setting during the hydrolysis process was neutral (pH=7). Enzyme inactivation was carried out at a temperature of 80°C for 20 min. Then, samples were centrifuged at 5000 rpm for 20 min, at 4°C, to obtain a fraction of the yellow tomalley hydrolysate of BSC.

Chemical profile screening. The experiment was carried out on an HP 6890 GCMS system (Hewlett-Packard, California, USA) with a capillary column (Agilent 19091S-433 HP-5MS; 30x250 m i.d.; Santa-Clara, California, USA). The carrier gas was helium, with a 1 mL min^{-1} flow rate. The oven was preheated to 325°C. The pre-oven temperature was set to 150°C and maintained at a 2°C min^{-1} rate. It ran at 10°C min^{-1} for 10 min before increasing to 240°C for 11 min. Running took at least 24 min (Riyadi et al 2021b). The scanning range was between 50 and 550 amu. The quantification of the predicted compound was obtained from reading the area on the GC-MS graph. The compound estimation results from the GC-MS test were carried out using the Wiley/NIST Library software (Tanod et al 2019).

Computational analysis. The initial step was to get canonical SMILE data of small molecules from YTHBSC from the PubChem server (https://pubchem.ncbi.nlm.nih.gov/) (Kim et al 2016b). The second step was predicting the biological activity of small molecules using the PASS server (http://www.way2drug.com/PASSOnline/predict.php) by inputting canonical SMILE data (Riyadi et al 2020c). The PASS online could predict over 300 pharmacological properties and biochemical pathways (Lagunin et al 2000; Dai et al 2016). The prediction is analyzed according to structure-activity interactions in the experimental dataset, containing information on over 300000 organic compounds (Filimonov et al 2014). Then, a list of the biological activity of small molecules was obtained from this server along with the Pa (to be active) and Pi (to be inactive) values. Pa value was set at >0.5. The higher Pa value indicates the high probability activity of the small molecule.

SwissADME (http://www.swissadme.ch/) was used to estimate drug-likeness, excretion, metabolism, distribution, and absorption (Christina et al 2021). The

physicochemical ranges on each axis were calculated using the swissADME software and shown as pink areas where the molecular radar plot must fall to be classified as drug-like or nutraceutical (Gupta et al 2022). SwissADME offers five free models for determining a compound's lipophilicity character: XLOGP3, WLOGP, MLOGP, SILICOS-IT, and iLOGP. XLOGP3, a knowledge-based library and an atomistic approach with corrective features (Tripathi et al 2019). WLOGP is a purely atomistic method for dealing with a fragmented system (Chandran et al 2019). MLOGP is a topological approach archetype that employs 13 molecular descriptors and a linear relationship (Eros et al 2002). SILICOS-IT is a hybrid approach that employs 7 topological descriptors and 27 fragments. In iLOGP, solvation-free energies in n-octanol and water are determined using the generalized-born and solvent-accessible surface area (GB/SA) model. The log P o/w is the mean of the values projected from 5 suggested approaches (Daina et al 2017). The findings were calculated using Open babel v 2.3.0 (O'Boyle et al 2011). The PSA is computed by applying the polar atoms sulfur and phosphorus and a fragmental technique known as TPSA or topological polar surface area (Ertl et al 2000). The Egan egg is an elliptical region populated by well-absorbed molecules that was utilized to test the model's efficacy for GI passive absorption and prediction of brain access via passive diffusion to lay the BOILED-Egg (Brain or intestinal estimated permeation predictive model). The Lipinski rule is the first of 5 guidelines for identifying tiny compounds according to physicochemical parameter profiles such NH or OH≤5, molecular weight less than 500, N or O≤10 and MLOGP≤4.15 (Raschka et al 2018). ProTox II (https://tox-new.charite.de/protox II/index.php?site=compound input) was used to determine toxicity of small molecules from YTHBSC (Riyadi et al 2020d).

Results and Discussion. The small molecule profiling in the YTHBSC was analyzed using GC-MS. Based on the GC-MS analysis, there were nine small molecules in YTHBSC. Table 1 presents that the major small molecule of YTHBSC was 4-(2-aminoethyl)-phenol, indicated by the highest percentage of the area (47.14%), with a retention time of 12.690 min. The other small molecules of YTHBSC were benzeneethanamine (14.98 %), pyridine (12.30 %) and N,N-dimethyl-methanamine (11.65%). The percentages of the area of other small molecules less than 10% were 2-piperidinone (8.94%), 2.5-dimethyl-1H-pyrrole (2.27%), decahydro-4H-cyclopentacycloocten-4-one (1.61%), and 2-(1H-tetrazole -5-yl)-pyridine (1.09%).

Table 1

Profile of small molecules from YTHBSC analyzed by GC-MS

No	*Small molecule*	*Molecular formula*	*Retention time (Min)*	*Area (%)*	*Quality (Min 50)*	*Library*	*Pubchem ID*
1	2-(1H-tetrazol-5-yl)-Pyridine	$C_6H_5N_5$	1.432	1.09	59	Wiley275.L	320267
2	N,N-dimethyl-Methanamine	C_3H_9N	1.500	11.65	80	Wiley275.L	1146
3	Pyridine	C_5H_5N	2.741	9.73	72	Wiley275.L	1049
4	Pyridine	C_5H_5N	3.094	2.57	58	Wiley275.L	1049
5	2,5-dimethyl-1H-Pyrrole	C_6H_9N	3.974	2.27	52	Wiley275.L	12265
6	Benzeneethanamine	$C_8H_{11}N$	7.933	14.98	90	NIST02.L	1001
7	2-Piperidinone	C_5H_9NO	9.259	8.94	64	Wiley275.L	12665
8	4-(2-aminoethyl)-Phenol	$C_8H_{11}N$	12.690	47.14	90	NIST02.L	5610
9	decahydro-4H-Cyclopentacycloocten-4-one	$C_{11}H_{18}N$	20.773	1.61	64	Wiley275.L	558671

After identifying the small molecules of YTHBSC, the next step was to predict their biological activity using the PASS online program. Table 2 presents the prediction of the biological potential of small molecules of YTHBSC as antihypertensive agents using PASS

online. Several antihypertensive effects of YTHBSC small molecule were predicted, including loop diuretics, antiadrenergic drugs, antihypertensive vasodilators, renin-angiotensin-aldosterone blockers, and antagonist receptor angiotensin 2 (Table 2). 2-(1H-tetrazol-5-yl)-pyridine has a potential as an angiotensin AT1A receptor antagonist (Pa 0.866), angiotensin AT1 receptor antagonist (Pa 0.859), Angiotensin II receptor antagonist (Pa 0.856), and angiotensin antagonist (Pa 0.854). The major small molecules of 4-(2-aminoethyl)-phenol possessed GABA C receptor activity (Pa 0.749), while benzeneethanamine, the second major small molecule of YTHBSC, had antineuritic activity (Pa 0.728) (Table 2).

Physicochemical properties of small molecules of YTHBSC were used to determine their possible role in various chemical, biological and physical processes. The molecular weight and polarity of 4-(2-aminoethyl)-phenol were 137.18 g mol^{-1} and 46.25 Å2, respectively (Table 3). The molecular weight and polarity of benzeneethanamine were 121.18 g mol^{-1} and 26.02 Å2, respectively. The molecular weight and polarity of 2-(1H-tetrazole -5-yl)-pyridine and decahydro-4H-cyclopentacycloocten-4-one were 147.14 and 1566.26 g mol^{-1}, and 67.35 and 17.07 Å2, respectively. Based on these results, 4-(2-aminoethyl)-phenol, benzeneethanamine, 2-(1H-tetrazole -5-yl)-pyridine and decahydro-4H-cyclopentacycloocten-4-one meet the optimum criteria of their physicochemical properties.

Table 2

Small molecule from YTHBSC with Pa value higher than 0.5 using PASS online

No	*Small molecule*	*PASS Online*		
		Pa	*Pi*	*Activity*
1	2-(1H-tetrazol-5-yl)-Pyridine	0.866	0.002	Angiotensin AT1A receptor antagonist
		0.859	0.001	Angiotensin AT1 receptor antagonist
		0.856	0.001	Angiotensin II receptor antagonist
		0.854	0.001	Angiotensin antagonist
2	N,N-dimethyl-Methanamine	0.612	0.004	Loop diuretic
3	Pyridine	0.620	0.004	Loop diuretic
4	2,5-dimethyl-1H-Pyrrole	0.637	0.008	Antihypertensive
5	Benzeneethanamine	0.728	0.033	Antineurotic
6	2-Piperidinone	0.716	0.033	GABA C receptor agonist
7	4-(2-aminoethyl)-Phenol	0.749	0.003	GABA C receptor agonist
8	decahydro-4H-Cyclopentacycloocten-4-one	0.657	0.014	Vasoprotector

Table 3

Physicochemical properties of the small molecule from YTHBSC

Small molecule	*MW*	*HA*	*AHA*	*RB*	*HBA*	*HBD*	*MR*	*TPSA*
2-(1H-tetrazol-5-yl)-pyridine	147.14	11	11	1	4	1	37.41	67.35
N,N-dimethyl-methanamine	59.11	4	0	0	1	0	19.43	3.24
Pyridine	79.10	6	6	0	1	0	24.24	12.89
2,5-dimethyl-1H-Pyrrole	95.14	7	5	0	0	1	30.72	15.79
Benzeneethanamine	121.18	9	6	2	1	1	38.92	26.02
2-Piperidinone	99.13	7	0	0	1	1	30.95	29.10
4-(2-aminoethyl)- phenol	137.18	10	6	2	2	2	40.95	46.25
Decahydro-4H-cyclopentacycloocten-4-one	166.26	12	0	0	1	0	50.96	17.07

Note: MW - molecular weight (g mol^{-1}); HA – number heavy atoms; AHA – number aromatic heavy atoms; RB – number rotatable bonds; HBA – number hydrogen bond acceptor; HBD – number hydrogen bound donor; MR - molar refractivity (m^3 mol^{-1}); TPSA - topology polar surface area ($Å^2$).

The XLOGP3 of 4-(2-aminoethyl)-phenol and benzeneethanamine were 1.10 and 1.41, respectively. It was indicated that lipophilicity ranged between -0.7 and +5.0 (Table 4).

Table 4

Lipophilicity characteristics of the small molecule from YTHBSC

Small molecule	*iLOGP*	*XLOGP3*	*WLOGP*	*MLOGP*	*SILICOS-IT*	*Consensus Log P*
2-(1H-tetrazol-5-yl)-Pyridine	0.59	0.10	0.26	0.20	1.18	0.47
N,N-dimethyl-Methanamine	1.56	0.26	1.18	0.29	-0.58	0.34
Pyridine	1.32	0.65	1.08	0.41	1.63	1.02
2,5-dimethyl-1H-Pyrrole	1.62	1.51	1.63	0.84	2.35	1.59
Benzeneethanamine	1.72	1.41	1.19	1.87	1.79	1.60
2-Piperidinone	1.28	-0.46	-0.09	0.10	1.32	0.43
4-(2-aminoethyl)- Phenol	1.36	1.10	0.89	1.21	1.28	1.17
Decahydro-4H-Cyclopentacycloocten-4-one	2.34	3.17	2.94	2.59	2.98	2.80

Table 5 presents the water solubility characteristics of the small molecule from YTHBSC. The results revealed that the primary compounds found in the YTHBSC have high solubility. The pharmacokinetic parameters, bioavailability, and drug-likeness were also assessed (Tables 6 and 7). There are 6 out of 8 small molecules of YTHBSC that have good bioavailability (Table 6). Bioavailability is an essential aspect to consider while developing nutraceuticals.

Table 5

Water solubility characteristics of the small molecule from YTHBSC

Compounds	*Log S*	*Solubility*		*Class*
		mg mL^{-1}	*mol L^{-1}*	
2-(1H-tetrazol-5-yl)-pyridine	-1.07	1.25e+01	8.52e-02	Very soluble
N,N-dimethyl-methanamine	0.11	7.63e+01	1.29e+00	Highly soluble
Pyridine	-0.50	2.52e+01	3.19e-01	Very soluble
2,5-dimethyl-1H-pyrrole	-1.45	3.38e+00	3.55e-02	Very soluble
Benzeneethanamine	-1.56	3.33e+00	2.75e-02	Very soluble
2-piperidinone	0.32	2.05e+02	2.07e+00	Highly soluble
4-(2-aminoethyl)- phenol	-1.66	2.97e+00	2.17e-02	Very soluble
Decahydro-4H-cyclopentacycloocten-4-one	-3.20	1.05e-01	6.32e-04	Soluble

Note: insoluble < -10 < poorly soluble < -6 < moderately soluble < -4 < soluble < -2 very soluble < 0 < highly soluble.

Table 6

Pharmacokinetics parameters and bioavailability of the small molecule from YTHBSC

Small molecule	*GI absorption*	*BBB permeant*	*Bioavailability score*
2-(1H-tetrazol-5-yl)-pyridine	High	No	0.85
N,N-dimethyl-methanamine	Low	No	0.55
Pyridine	High	Yes	0.55
2,5-dimethyl-1H-pyrrole	High	Yes	0.55
Benzeneethanamine	High	Yes	0.55
2-piperidinone	High	No	0.55
4-(2-aminoethyl)- phenol	High	Yes	0.55
decahydro-4H-cyclopentacycloocten-4-one	High	Yes	0.55

Note: GI absorption - gastrointestinal absorption; BBB permeant – blood brain barrier permeation.

Table 7

Drug likeness rule score of the small molecule from YTHBSC

Small molecule	*A*	*B*	*C*	*D*	*E*
2-(1H-tetrazol-5-yl)-Pyridine	Yes	Yes	Yes	Yes	Yes
N,N-dimethyl-Methanamine	Yes	Yes	Yes	Yes	Yes
Pyridine	Yes	Yes	Yes	Yes	Yes
2,5-dimethyl-1H-Pyrrole	Yes	Yes	Yes	Yes	Yes
Benzeneethanamine	Yes	Yes	Yes	Yes	Yes
2-Piperidinone	Yes	Yes	Yes	Yes	Yes
4-(2-aminoethyl)- Phenol	Yes	Yes	Yes	Yes	Yes
decahydro-4H-Cyclopentacycloocten-4-one	Yes	Yes	Yes	Yes	Yes

Note: A - molecular mass less than 500 Dalton; B - high lipophilicity (expressed as LogP less than 5); C - less than 5 hydrogen bond donors; D - less than 10 hydrogen bond acceptors; E - molar refractivity should be between 40-130; F - conclusion.

According to the bioavailability radar (Figure 1), the colorful zone is the best physicochemical area for oral bioavailability.

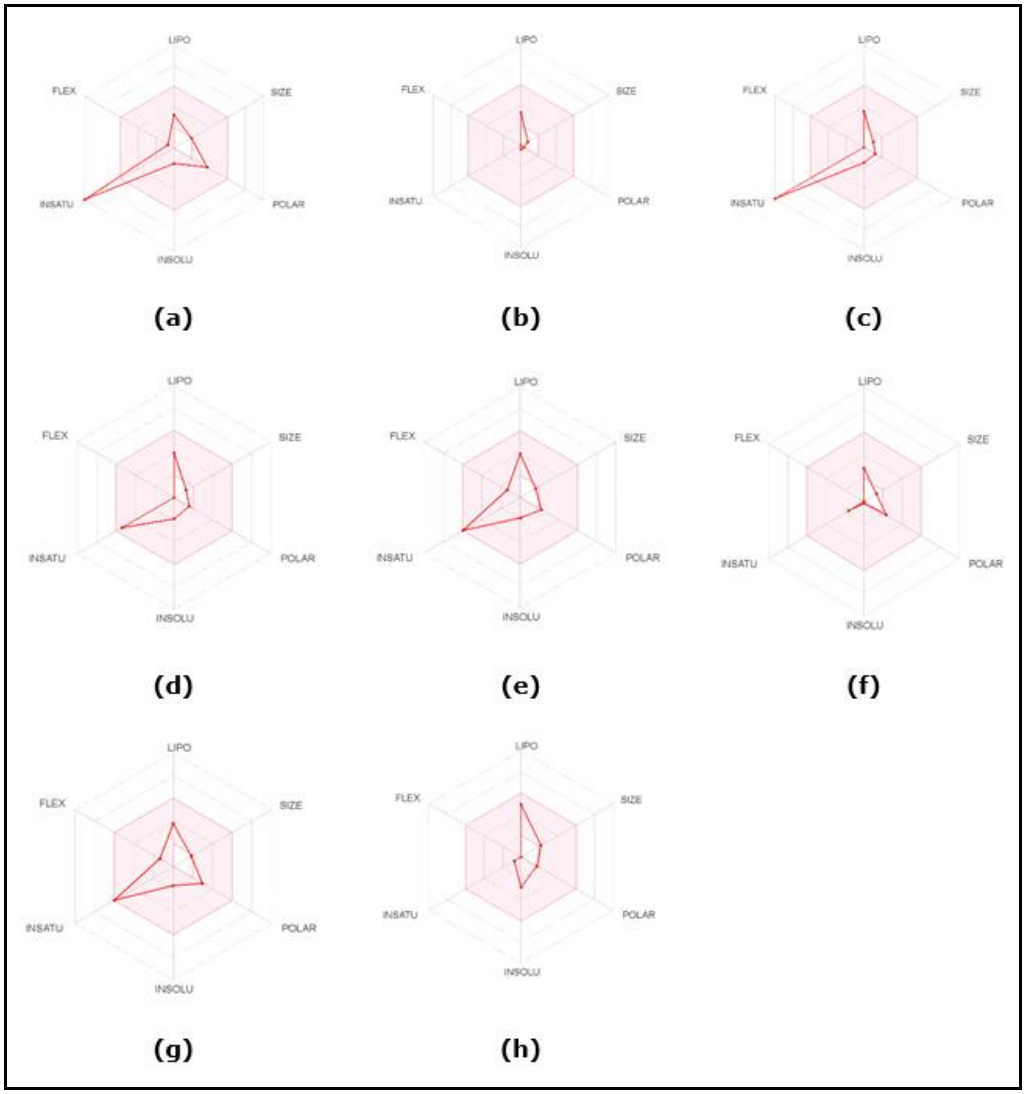

Figure 1. Schematic diagram of the bioavailability radar for drug likeness of the small molecule from YTHBSC: (a) 2-(1H-tetrazol-5-yl)-pyridine; (b) N,N-dimethyl-methanamine; (c) pyridine; (d) 2,5-dimethyl-1H-pyrrole; (e) benzeneethanamine; (f) 2-piperidinone; (g) 4-(2-aminoethyl)- phenol; (h) decahydro-4H-cyclopentacycloocten-4-one.

Eight small molecules had a molecular mass of less than 500 Dalton, high lipophilicity, less than 5 hydrogen bond donors, less than 10 hydrogen bond acceptors, and molar refractivity between 40-130 (Table 7). All small molecules from YTHBSC have a value between 1 and 2.47, making them easy to produce synthetically (Table 8). Table 9 presents oral toxicity prediction results from the small molecule of YTHBSC. N,N-dimethyl-methanamine, and 2-piperidinone belong to class II (fatal if swallowed; 5<LD50≤50) and were based on ProTo-II. Mutagenicity and cytotoxicity prediction results from all small molecules of YTHBSC were negative.

Table 8

Medicinal chemistry prediction of the small molecule from YTHBSC

Small molecule	*A*	*B*	*C*	*D*
2-(1H-tetrazol-5-yl)-pyridine	No; 1 violation; MW<250	0	0	1.83
N,N-dimethyl-methanamine	No; 1 violation; MW<250	0	0	1.00
Pyridine	No; 1 violation; MW<250	0	0	1.00
2,5-dimethyl-1H-pyrrole	No; 1 violation; MW<250	0	0	1.00
Benzeneethanamine	No; 1 violation; MW<250	0	0	1.00
2-piperidinone	No; 1 violation; MW<250	0	0	1.00
4-(2-aminoethyl)- phenol	No; 1 violation; MW<250	0	0	1.00
decahydro-4H-cyclopentacycloocten-4-one	No; 1 violation; MW<250	0	0	2.47

Note: A – lead likeness; B – pan assay interference structures; C – structural alert; D – synthetic accessibility score.

Table 9

Oral toxicity prediction results from the small molecule of YTHBSC using ProTox II

Small molecule	*LD50*	*Class*	*HE*	*CA*	*IM*	*MU*	*CY*
2-(1H-tetrazol-5-yl)-pyridine	1190	4	(+)	(-)	(+)	(-)	(-)
N,N-dimethyl-methanamine	50	2	(-)	(-)	(-)	(-)	(-)
Pyridine	1500	4	(-)	(+)	(-)	(-)	(-)
2,5-dimethyl-1H-pyrrole	670	4	(-)	(+)	(-)	(-)	(-)
Benzeneethanamine	400	4	(-)	(-)	(-)	(-)	(-)
2-piperidinone	41	2	(-)	(-)	(-)	(-)	(-)
4-(2-aminoethyl)- phenol	1090	4	(-)	(-)	(-)	(-)	(-)
decahydro-4H-cyclopentacycloocten-4-one	25	2	(-)	(-)	(-)	(-)	(-)

Note: LD50 - lethal dose 50% of response (mg kg^{-1}); HE - hepatotoxicity; CA - carcinogenicity; IM - immunotoxiticity; MU - mutagenicity; CY - cytotoxicity; (-) - inactive; (+) - active; class 1 - fatal if swallowed (LD50≤5); class 2 - fatal if swallowed (5<LD50≤50); class 3 - toxic if swallowed (50<LD50≤300); class 4 - harmful if swallowed (300<LD50≤2000); class 5 - may be harmful if swallowed (2000<LD50≤5000); class 6 - non-toxic (LD50>5000).

The results showed that the highest Pa value was found in 2-(1H-tetrazol-5-yl)-pyridine, which has potential activity as an angiotensin receptor antagonist. Benzeneethanamine has the potential as an antineurotic, and 2-piperidinone and 4-(2-aminoethyl)-phenol act as GABA C receptor agonists (Table 2). Pyridine was the most prevalent structural unit due to its versatility for drug development against many biological targets. The dihydropyridine ring mostly acts as a calcium-channel blocker, which has advantages for hypertension and heart-related disease treatment (Ling et al 2021). Another compound,

N,N-dimethyl-methanamine was also reported to have a negative association with high blood pressure (Hsu et al 2020), while the 2-piperidinone and its derivative might be used to develop an antihypertensive agent (Yang et al 2007).

The molecular and physicochemical activity such as molecular weight, molecular formula, H-bond donors, H-bond acceptors, rotatable bonds, heavy aromatic atoms, heavy atoms, molar refractivity, and TPSA are among the physicochemical properties of YTHBSC small molecules (Table 3). The YTHBSC small molecules' general features revealed that the molecular weight of all compounds was less than 500 Da, indicated as a key attribute that can be referred to as drug-likeness. The lipophilicity properties of the YTHBSC small molecules are shown in Table 4.

The amount of nutraceutical dosage can be reduced if the bioavailability is good. Furthermore, it can lower the danger of side effects and toxicity, while achieving the target pharmacological effect. Poor bioavailability can lead to decreased efficacy and greater inter-individual variability, resulting in an unanticipated reaction to a nutraceutical. Nutraceutical candidates fail to reach the market because of poor bioavailability in clinical trials. Anacardic acid is one of the 15 insoluble chemicals. One of the methods used by Ali et al (2012) to estimate water solubility was SwissADME (Solubility class: Log S Scale: Insoluble < -10 poorly <-6, moderately < -4 soluble< -2 very < 0 < highly). The solvent used, ambient temperature, and pressure significantly impact a compound's solubility. The saturated level is the point in an optimizer concentration in which adding more solute has no impact (Savjani et al 2012). The GI absorption of all YTHBSC small molecules was high, except N,N-dimethyl-methanamine (Table 6). This suggests that most of the YTHBSC small molecules have good absorption. According to Lipinski's rules, all small molecules from YTHBSC matched the drug-likeness criteria (Table 7).

The Lilly MedChem (Bruns & Watson 2012) rule used to purify chemical libraries of compounds that are likely to be unstable, reactive, toxic, or prone to interfere with biological assays due to their structure has been based on the root of structural alert (Brenk et al 2008), the pan assay interference compounds or PAINS structural alert (Baell & Holloway 2010), or the root of structural alert (Brenk et al 2008; Irwin et al 2015). The synthetic accessibility (SA) score is predicated on the concept that the frequency of molecular fragments in 'really' available compounds relates to synthesis ease. Ertl & Schuffenhauer (2009) reported the created and validated method as being characterized by the molecular synthetic accessibility value, which varied from 1 to 10 (easy to very difficult).

Drug-induced hepatotoxicity is a primary cause of abrupt liver failure and one of the leading causes of drug rejections (Siramshetty et al 2016; Banerjee et al 2018). Drug-induced liver injury (DILI) might be long-term or occur only once. The ProTox-II hepatotoxicity prediction model has equitable reliability of 82% on cross-validation and an accuracy of 86% on external validation (Chen et al 2016).

Conclusions. The current study suggested that small molecules from the yellow tomalley hydrolysate of BSC may have the potential as antihypertensive agents. Six to eight small molecules met the pharmacokinetic criteria. Further research should be done in vitro and in vivo to elucidate the small molecules from YTHBSC, which might be used as an antihypertensive agent and further develop excellent nutraceutical products.

Acknowledgements. This research was funded by the Universitas Diponegoro through the International Publication of Research Program with grant no. SPK: 185-73/UN7.6.1/PP/2022.

Conflict of Interest. The authors declare that there is no conflict of interest.

References

Ali J., Camilleri P., Brown M. B., Hutt A. J., Kirton S. B., 2012 Revisiting the general solubility equation: in silico prediction of aqueous solubility incorporating the effect

of topographical polar surface area. Journal of Chemical Information and Modeling 52(2):420-428.
Baell J. B., Holloway G. A., 2010 New substructure filters for removal of pan assay interference compounds (PAINS) from screening libraries and for their exclusion in bioassays. Journal of Medicinal Chemistry 53(7):2719-2740.
Banerjee P., Eckert A. O., Schrey A. K., Preissner R., 2018 ProTox-II: a webserver for the prediction of toxicity of chemicals. Nucleic Acids Research 46(W1):W257-W263.
Brenk R., Schipani A., James D., Krasowski A., Gilbert I. H., Frearson J., Wyatt P. G., 2008 Lessons learnt from assembling screening libraries for drug discovery for neglected diseases. ChemMedChem 3(3):435-444.
Bruns R. F., Watson I. A., 2012 Rules for identifying potentially reactive or promiscuous compounds. Journal of Medicinal Chemistry 55(22):9763-9772.
Chandran A., Merlin N. J., Ammu L., Dharan S. S., 2019 Fennel treatment to PCOS: An insilico evaluation to explore the therapeutic efficacy of anethole. Research Journal of Pharmacy and Technology 12(10):4958-4962.
Chang J. B., Lee Y., 2019 The effects of technological development on fisheries production. Fisheries Science 85:259-269.
Chen M., Suzuki A., Thakkar S., Yu K., Hu C., Tong W., 2016 DILIrank: the largest reference drug list ranked by the risk for developing drug-induced liver injury in humans. Drug Discovery Today 21(4):648-653.
Christina Y. I., Nafisah W., Atho'illah M. F., Rifa'i M., Widodo N., Djati M. S., 2021 Anti-breast cancer potential activity of *Phaleria macrocarpa* (Scheff.) Boerl. leaf extract through in silico studies. Journal of Pharmacy & Pharmacognosy Research 9(6):824-845.
Dai S. X., Li W. X., Han F. F., Guo Y. C., Zheng J. J., Liu J. Q., Wang Q., Gao Y. D., Li G. H., Huang J. F., 2016 In silico identification of anti-cancer compounds and plants from traditional Chinese medicine database. Scientific Reports 6:25462.
Daina A., Michielin O., Zoete V., 2017 SwissADME: a free web tool to evaluate pharmacokinetics, drug-likeness and medicinal chemistry friendliness of small molecules. Scientific Reports 7:42717.
Eros D., Kövesdi I., Orfi L., Takács-Novák K., Acsády G., Kéri G., 2002 Reliability of logP predictions based on calculated molecular descriptors: a critical review. Current Medicinal Chemistry 9(20):1819-1829.
Ertl P., Rohde B., Selzer P., 2000 Fast calculation of molecular polar surface area as a sum of fragment-based contributions and its application to the prediction of drug transport properties. Journal of Medicinal Chemistry 43(20):3714-3717.
Ertl P., Schuffenhauer A., 2009 Estimation of synthetic accessibility score of drug-like molecules based on molecular complexity and fragment contributions. Journal of Cheminformatics 1:8.
Filimonov D. A., Lagunin A. A., Gloriozova T. A., Rudik A. V., Druzhilovskii D. S., Pogodin P. V., Poroikov V. V., 2014 Prediction of the biological activity spectra of organic compounds using the PASS online web resource. Chemistry of Heterocyclic Compounds 50(3):444-457.
Gao R., Yu Q., Shen Y., Chu Q., Ge C., Fen S., Yang M., Yuan L., McClements D. J., Sun Q., 2021 Production, bioactive properties, and potential applications of fish protein hydrolysates: Developments and challenges. Trends in Food Science & Technology 110:687-699.
Gupta A., Ahmad R., Siddiqui S., Yadav K., Srivastava A., Trivedi A., Ahmad B., Khan M. A., Shrivastava A. K., Singh G. K., 2022 Flavonol morin targets host ACE2, IMP-α, PARP-1 and viral proteins of SARS-CoV-2, SARS-CoV and MERS-CoV critical for infection and survival: a computational analysis. Journal of Biomolecular Structure and Dynamics 40(12):5515-5546.
Hsu C. N., Chang-Chien G. P., Lin S., Hou C. Y., Lu P. C., Tain Y. L., 2020 Association of trimethylamine, trimethylamine N-oxide, and dimethylamine with cardiovascular risk in children with chronic kidney disease. Journal of Clinical Medicine 9(2):336.

Irwin J. J., Duan D., Torosyan H., Doak A. K., Ziebart K. T., Sterling T., Tumanian G., Shoichet B. K., 2015 An aggregation advisor for ligand discovery. Journal of Medicinal Chemistry 58(17):7076-7087.
Kim S. B., Yoon N. Y., Shim K. B., Lim C. W., 2016b Antioxidant and angiotensin I-converting enzyme inhibitory activities of northern shrimp (*Pandalus borealis*) by-products hydrolysate by enzymatic hydrolysis. Fisheries and Aquatic Sciences 19:29.
Kim S., Thiessen P. A., Bolton E. E., Chen J., Fu G., Gindulyte A., Han L., He J., He S., Shoemaker B. A., Wang J., Yu B., Zhang J., Bryant S.H., 2016a PubChem substance and compound databases. Nucleic Acids Research 44(D1):D1202-D1213.
Lagunin A., Stepanchikova A., Filimonov D., Poroikov V., 2000 PASS: prediction of activity spectra for biologically active substances. Bioinformatics 16(8):747-748.
Ling Y., Hao Z. Y., Liang D., Zhang C. L., Liu Y. F., Wang Y., 2021 The expanding role of pyridine and dihydropyridine scaffolds in drug design. Drug Design, Development, and Therapy 15:4289-4338.
Mensah G. A., 2016 Hypertension and target organ damage: don't believe everything you think! Ethnicity & Disease 26(3):275-278.
Mills K. T., Stefanescu A., He J., 2020 The global epidemiology of hypertension. Nature Reviews. Nephrology. 16(4):223-237.
Ndombera F., Maiyoh G., Tuei V., 2019 Pharmacokinetic, physicochemical and medicinal properties of N-glycoside anti-cancer agent more potent than 2-deoxy-D-glucose in lung cancer cells. Journal of Pharmacy and Pharmacology 7(4):165-176.
O'Boyle N. M., Banck M., James C. A., Morley C., Vandermeersch T., Hutchison G. R., 2011 Open Babel: An open chemical toolbox. Journal of Cheminformatics 3:33.
Raschka S., Wolf A. J., Bemister-Buffington J., Kuhn L. A., 2018 Protein–ligand interfaces are polarized: discovery of a strong trend for intermolecular hydrogen bonds to favor donors on the protein side with implications for predicting and designing ligand complexes. Journal of Computer-aided Molecular Design 32(4):511-528.
Riyadi P. H., Atho'illah M. F., Tanod W. A., Rahmawati, I. S., 2020b Tilapia viscera hydrolysate extract alleviates oxidative stress and renal damage in deoxycorticosterone acetate-salt-induced hypertension rats. Veterinary World 13(11):2477-2483.
Riyadi P. H., Darmanto Y. S., Anggo A. D., Sumardianto S., Rianingsih L., 2020a Color test for screening chemical components of protein hydrolyzed extract from non-shell small crab (*Portunus Pelagicus*) waste. International Journal Science and Technology Research 9(5):6-9.
Riyadi P. H., Romadhon R., Anggo A. D., Herawati V. E., Setyastuti A. I., 2020d PASS and ADMET analyses for eight compounds from Nile tilapia (*Oreochromis niloticus*) viscera waste hydrolysate as anti-inflammatory nutraceutical. AACL Bioflux 13(5):2630-2638.
Riyadi P. H., Suprayitno E., Sulistiati T. D., 2019 Optimization of protein hydrolysate from visceral waste of Nile tilapia (*Oreochromis niloticus*) by response surface methodology. AACL Bioflux 12(6):2347-2358.
Riyadi P. H., Tanod W. A., Dewanto D. K., Herawati V. E., Susanto E., Aisiah S., 2021b Chemical profiles and antioxidant properties of Bruguiera gymnorrhiza fruit extracts from Central Sulawesi, Indonesia. Food Research 5(S3):37-47.
Riyadi P. H., Tanod W. A., Sulistiyati D. T., Aulanni'am A. A., Suprayitno E., 2021a Effects of nile tilapia (*Oreochromis niloticus*) viscera hydrolysate on blood pressure, TNF-α and IL-6 expression in rats (*Rattus norvegicus*) induced by DOCA-salt. Indian Journal of Animal Research 55(1):19-24.
Riyadi P. H., Tanod W. A., Wahyudi D., Susanto E., Fahmi A. S., Aisiah S., 2020c Potential of tilapia (*Oreochromis niloticus*) viscera bioactive peptides as antiviral for SARS-CoV-9 2 (COVID 19). IOP Conference Series: Earth and Environmental Science 584:012004.
Sasongko A. Y., Dewi E. N., Amalia, U., 2018 The utilization of blue swimming crab (*Portunus pelagicus*) waste product, Lemi, as a food flavor. IOP Conference Series: Earth and Environmental Science 102:012030.

Savjani K. T., Gajjar A. K., Savjani J. K., 2012 Drug solubility: importance and enhancement techniques. International Scholarly Research Notices 2012:195727.
Siramshetty V. B., Nickel J., Omieczynski C., Gohlke B. O., Drwal M. N., Preissner R., 2016 WITHDRAWN—a resource for withdrawn and discontinued drugs. Nucleic Acids Research 44(D1):D1080-D1086.
Sliwoski G., Kothiwale S., Meiler J., Lowe E. W., 2014 Computational methods in drug discovery. Pharmacological Reviews 66(1):334-395.
Tanod W. A., Dewanto D. K., Ndobe S., Riyadi P. H., Putra M. Y., 2019 Screening of antibacterial and antioxidant activity of soft corals *Sinularia* sp. and *Sarcophyton* sp. from Palu Bay Central Sulawesi. Squalen: Bulletin of Marine and Fisheries Postharvest and Biotechnology 14:73-83.
Tripathi P., Ghosh S., Talapatra S. N., 2019 Bioavailability prediction of phytochemicals present in *Calotropis procera* (Aiton) R. Br. by using Swiss-ADME tool. World Scientific News 131:147-163.
Vijaykrishnaraj M., Prabhasankar P., 2015 Marine protein hydrolysates: their present and future perspectives in food chemistry–a review. RSC Advances 5:34864-34877.
Zamora-Sillero J., Gharsallaoui A., Prentice C., 2018 Peptides from fish by-product protein hydrolysates and its functional properties: An overview. Marine Biotechnology 20(2):118-130.
Zloh M., Kirton S. B., 2018 The benefits of in silico modeling to identify possible small-molecule drugs and their off-target interactions. Future Medicinal Chemistry 10(4):423-432.
*** http://www.swissadme.ch/
*** http://www.way2drug.com/PASSOnline/predict.php
*** https://pubchem.ncbi.nlm.nih.gov/
*** https://tox-new.charite.de/protox II/index.php?site=compound input
*** Statistics Indonesia, 2021 [Export and import]. Available at: https://www.bps.go.id/exim/. [In Indonesian].
*** Yang J. C., Wang N., Yang X., Ren J. P., 2007 *Marasmius androsaceus* l.es fr extract, piperidone derivative, and their use for the preparation of antihypertensives. US patent application publication no: US2007/0160625A1.

Received: 29 May 2022. Accepted: 20 July 2022. Published online: 17 November 2022.
Authors:
Putut Har Riyadi, Department of Fish Products Technology, Faculty of Fisheries and Marine Sciences, Diponegoro University, Semarang 50275, Central Java, Indonesia, e-mail: putut.riyadi@live.undip.ac.id
Eko Susanto, Department of Fish Products Technology, Faculty of Fisheries and Marine Sciences, Diponegoro University, Semarang 50275, Central Java, Indonesia, e-mail: ekothp@live.undip.ac.id
Apri Dwi Anggo, Department of Fish Products Technology, Faculty of Fisheries and Marine Sciences, Diponegoro University, Semarang 50275, Central Java, Indonesia, e-mail: apri_thp@undip.ac.id
Mochammad Fitri Atho'illah, Department of Biology, Faculty of Mathematics and Natural Sciences, Brawijaya University, Malang 65145, East Java, Indonesia, e-mail: athoillah.mf@gmail.com
Muhaimin Rifa'i, Department of Biology, Faculty of Mathematics and Natural Sciences, Brawijaya University, Malang 65145, East Java, Indonesia, e-mail: rifa123@ub.ac.id

How to cite this article:
Riyadi P. H., Susanto E., Anggo A. D., Atho'illah M. F., Rifa'i M., 2022 Predicting drug-likeness properties of small molecules from yellow tomalley hydrolysate of blue swimming crab (*Portunus pelagicus*). AACL Bioflux 15(6):3027-3037.